2002

A Drift-Diffusion Equation for Ballistic Transport in Nanoscale Metal-Oxide-Semiconductor Field Effect Transistors

Jung-Hoon Rhew
Purdue University

Mark S. Lundstrom
Purdue University, lundstro@purdue.edu

Rhew, Jung-Hoon and Lundstrom, Mark S., "A Drift-Diffusion Equation for Ballistic Transport in Nanoscale Metal-Oxide-Semiconductor Field Effect Transistors" (2002). *Department of Electrical and Computer Engineering Faculty Publications.* Paper 121.
https://docs.lib.purdue.edu/ecepubs/121

Journal of Applied Physics

Drift-diffusion equation for ballistic transport in nanoscale metal-oxide-semiconductor field effect transistors

Cite as: Journal of Applied Physics **92**, 5196 (2002); https://doi.org/10.1063/1.1509098
Submitted: 04 March 2002 . Accepted: 26 July 2002 . Published Online: 21 October 2002

Jung-Hoon Rhew, and Mark S. Lundstrom

JOURNAL OF APPLIED PHYSICS VOLUME 92, NUMBER 9 1 NOVEMBER 2002

Drift-diffusion equation for ballistic transport in nanoscale metal-oxide-semiconductor field effect transistors

Jung-Hoon Rhew[a] and Mark S. Lundstrom
School of Electrical and Computer Engineering, 1285 EE Building, Purdue University, West Lafayette, Indiana 47907

(Received 4 March 2002; accepted 26 July 2002)

We develop a drift-diffusion equation that describes ballistic transport in a nanoscale metal-oxide-semiconductor field effect transistor (MOSFET). We treat injection from different contacts separately, and describe each injection with a set of extended McKelvey one-flux equations [Phys. Rev. **123**, 51 (1961); **125**, 1570 (1962)] that include hierarchy closure approximations appropriate for high-field ballistic transport and degenerate carrier statistics. We then reexpress the extended one-flux equations in a drift-diffusion form with a properly defined Einstein relationship. The results obtained for a nanoscale MOSFET show excellent agreement with the solution of the ballistic Boltzmann transport equation with no fitting parameters. These results show that a macroscopic transport model based on the moments of the Boltzmann transport equation can describe ballistic transport. © *2002 American Institute of Physics.* [DOI: 10.1063/1.1509098]

I. INTRODUCTION

As transistors are scaled down to their ultimate limit, carrier transport may approach the ballistic limit. This imposes a great challenge for predictive assessments of device performance, especially the on current of transistors, because (1) commonly used macroscopic transport models assuming collision-dominated transport are expected to lose their validity near the ballistic limit[1,2] and (2) computational burdens of reliable first-principles simulators (Monte Carlo simulators[3] or full Boltzmann solvers[4]) preclude them from routine use for extensive design studies. A macroscopic model derived from the moments of the Boltzmann transport equation (BTE) capable of describing carrier transport from the diffusive to the ballistic limit would be of great interest. Because conventional moment-based macroscopic models (e.g., drift-diffusion, or energy transport models) fail in the ballistic limit,[1,2] we turn our attention to McKelvey's one-flux method,[5,6] whose usefulness in qualitatively describing quasiballistic transport was demonstrated in the scattering theory.[7] But, the one-flux method is unable to describe carrier acceleration in a high-field region (e.g., the channel or the collector of a transistor).[8] In this article, we extend McKelvey's one-flux method and develop a drift-diffusion equation to describe pure ballistic transport in a nanoscale metal-oxide-semiconductor field effect transistor (MOSFET).

We solve the ballistic drift-diffusion equation for the model device shown in Fig. 1 and compare the results to the ballistic BTE solution obtained in Ref. 9. The model device is a 10-nm channel-length, double-gate MOSFET with an ultrathin body thickness of 1.5 nm. The gate oxides are 1.5 nm and both top and bottom gates have a midgap work function. The strong quantum confinement across the thin body provides two simplifying assumptions: (1) one subband model for which we assume all carriers are accommodated in the lowest subband and (2) quasi-two-dimensional (2D) simulation in which we solve one-dimensional (1D) transport along the body and a 1D Schrödinger equation across the body selfconsistently with a 2D Poisson equation.[9]

This article is organized as follows. In Sec. II, we examine the assumptions employed in the one-flux method. In Sec. III, we present the set of extended one-flux equations that can describe ballistic transport. In Sec. IV, we convert the extended one-flux equations into a drift-diffusion equation and solve in the ballistic limit for our model device, and compare the results against the solution of ballistic BTE. We then conclude in Sec. V.

II. MCKELVEY'S ONE-FLUX METHOD

Figure 2 illustrates the idea of McKelvey's one-flux method.[5,6] The two flux densities, $J^+(x)$ and $J^-(x+dx)$ (defined positively), incident on a semiconductor slab with thickness dx transmit or reflect with the backscattering probabilities per length, ξ and ξ', respectively, contributing to the outward fluxes $J^-(x)$ and $J^+(x+dx)$. This is described by the one-flux equations,[5,6] which are given as

$$\frac{dJ^+}{dx} = -\xi J^+ + \xi' J^-, \tag{2.1a}$$

$$\frac{dJ^-}{dx} = -\xi J^+ + \xi' J^-, \tag{2.1b}$$

where the backscattering probabilities per length are

$$\xi = \begin{cases} \xi_0 + \dfrac{q\varepsilon_x}{k_B T_L} & \varepsilon_x > 0 \\ \xi_0 & \varepsilon_x < 0 \end{cases}, \tag{2.1c}$$

---

[a] Electronic mail: rhew@ecn.purdue.edu

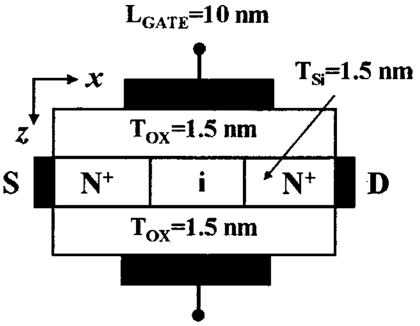

FIG. 1. The model, ultrathin-body double-gate MOSFET with 10 nm channel length. The source and drain regions are doped at 10^{20} cm^{-3}.

and
$$\xi'=\begin{cases}\xi_0 & \varepsilon_x>0\\ \xi_0-\dfrac{q\varepsilon_x}{k_BT_L} & \varepsilon_x<0\end{cases}. \tag{2.1d}$$

The low-field backscattering probability per length ξ_0 is associated with the low-field mobility μ_0 through Shockley's relation,[6] and T_L is the lattice temperature. See Appendix A for a brief derivation of Eqs. (2.1a)–(2.1d). The backscattering coefficients ξ and ξ' consist of two terms: (1) backscattering by actual scattering (ξ_0) and (2) backscattering by reflection from an *opposing* electric field (ε_x) as shown in Fig. 3. In Eqs. (2.1c) and (2.1d), the effect of actual scattering is assumed to be *symmetric* under a *low-field* condition.

By specifying the incoming fluxes at the boundaries, we can solve Eqs. (2.1) for $J^{\pm}$. However, to solve them self consistently with the Poisson equation, we need to know the carrier densities $n^{\pm}$ associated with $J^{\pm}$, which can be obtained by specifying the average velocities of ± streams, $\langle \nu_x\rangle^{\pm}$, because

$$J^{\pm}=n^{\pm}\langle \nu_x\rangle^{\pm}. \tag{2.2}$$

As in conventional moment equations, the average velocities are obtained in two ways (1) by solving the next order moment equations or (2) by employing hierarchy closure approximations.[10] The one-flux method closes the hierarchy by assuming $\langle \nu_x\rangle^{\pm}$ to be the average velocity of hemi-Maxwellian, i.e.,

$$\langle \nu_x\rangle^{\pm}\cong \nu_T=\sqrt{\frac{2k_BT_L}{\pi m^*}}. \tag{2.3}$$

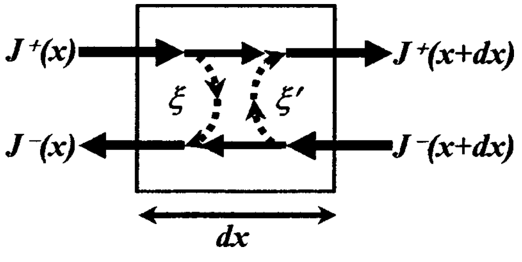

FIG. 2. Illustration of McKelvey's one-flux method. The two fluxes, $J^+(x)$ and $J^-(x+dx)$ are incident on a semiconductor slab with thickness dx, and transmit or backscatter inside with the backscattering probabilities per length, ξ and ξ', respectively.

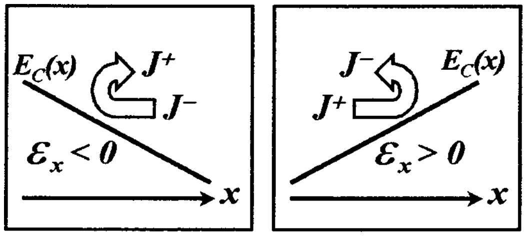

FIG. 3. Illustration of the effects of the opposing electric field.

Thanks to its flux description, the one-flux method successfully describes carrier transport from the diffusive to the ballistic limit when there is negligible acceleration, e.g., transport across a thin base.[11] However, the one-flux equations are derived from the zeroth moments of the BTE,[8] in which the numbers of carriers in streams do not change due to acceleration. Thus, the field terms describe only backscattering and are associated with hemi-Maxwellian distributions in nondegenerate conditions (see Appendix A). The effect of acceleration such as velocity overshoot should be cast into hierarchy closure approximations on $\langle \nu_x\rangle^{\pm}$, which is missing in Eq. (2.3). In conclusion, the one-flux method is valid under *nondegenerate* conditions with *negligible* acceleration.

III. EXTENDED ONE-FLUX METHOD FOR BALLISTIC MOSFETS

A. Separating injections, closure approximations, and degenerate statistics

Figure 4 shows types of transport in a nanoscale MOSFET. In the channel region after the source barrier, the + stream from the source (J_S^+) is accelerated by the electric field whereas the injection from the drain contact (J_D^-) is decelerated and backscattered. Different populations experience different types of transport in the same region. Therefore, it is natural to treat the source-injected fluxes separately from the drain-injected fluxes and then describe each injection with the one-flux equations as illustrated in Fig. 5. In other words, we solve one set of flux equations for the source-injected carriers and another for the drain-injected carriers. The total carrier density and the net current are the

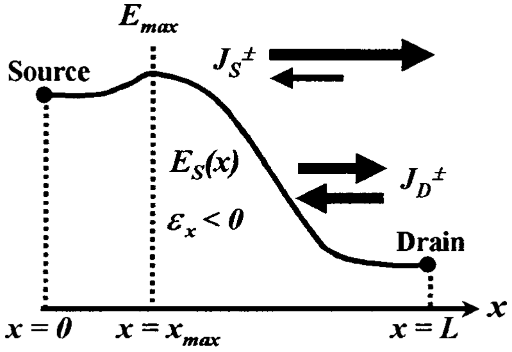

FIG. 4. Types of transport in a nanoscale MOSFET under bias. $E_{\max}$ is the maximum of the subband energy $E_S(x)$. In the channel region after the source barrier, J_S^+ is accelerated by the electric field whereas J_D^- is decelerated and backscattered.

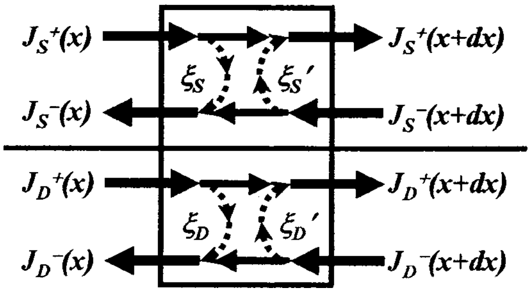

FIG. 5. Illustration of separation of carrier injections from the source and the drain.

sum of the quantities obtained for each injection. The idea of separating injections is based on the *linearity* of the ballistic BTE, which we can solve for the source injection and the drain injection separately and then obtain the final distribution as a superposition of the two. This approach enables us to apply different macroscopic approximations (scattering parameters and hierarchy closure assumptions) to sets of one-flux equations that describe different populations. It is obvious that we can use the original one-flux equations for streams under deceleration (e.g., drain-injected fluxes under bias), but new approximations are required to describe streams under acceleration. Another modification required for a nanoscale MOSFET is to include degenerate carrier statistics because they may affect the on current.[9] In the ballistic limit, we can implement degenerate statistics into each injection separately.

In conclusion, we will extend McKelvey's one-flux method by (1) treating carriers injected from the source and drain separately, (2) introducing hierarchy closure approximations for the streams under acceleration, and (3) including degenerate carrier statistics.

B. Ballistic one-flux equations with degeneracy for nanoscale MOSFETs

In the ballistic limit ($\xi_0=0$) with degenerate carrier statistics, the backscattering coefficients become (see Appendix B for a derivation.)

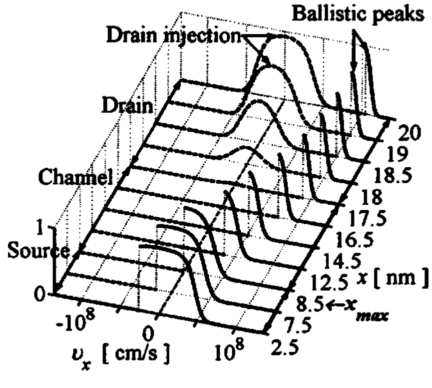

FIG. 6. Cross-sectional shapes of off-equilibrium distributions along the longitudinal direction (ν_x) at different locations in the device at $V_{GS}=V_{DS}=0.6$ V (from Ref. 9). The source injection (solid lines) develops into a ballistic peak approaching a delta function.

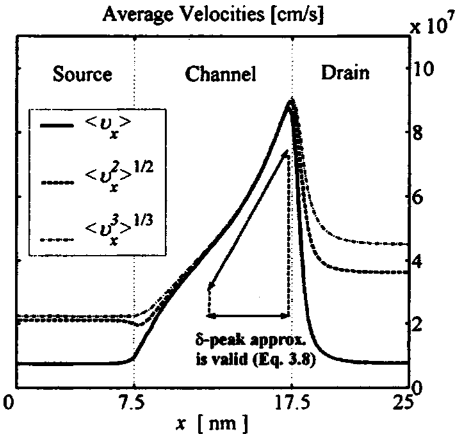

FIG. 7. The profiles of average velocities at the first-, second-, and the third-order moments in the ballistic limit. In the channel region where ballistic peaks develop in Fig. 6, Eq. (3.8) is a valid approximation.

$$\xi=\begin{cases} +\dfrac{q\varepsilon_x}{k_BT}F_{\text{deg}}^{+}(\eta_+) & \varepsilon_x>0 \\ 0 & \varepsilon_x<0 \end{cases}, \tag{3.1a}$$

and

$$\xi'=\begin{cases} 0 & \varepsilon_x>0 \\ -\dfrac{q\varepsilon_x}{k_BT}F_{\text{deg}}^{-}(\eta_-) & \varepsilon_x<0 \end{cases}. \tag{3.1b}$$

For 2D electrons in the lowest subband of our model device, the degeneracy factors are

$$F_{\text{deg}}^{\pm}(\eta_\pm)=\frac{\mathscr{F}_{-1/2}(\eta_\pm)}{\mathscr{F}_{1/2}(\eta_\pm)},\quad \text{for } \pm \text{stream}, \tag{3.2}$$

where $\mathscr{F}_{-1/2}$ and $\mathscr{F}_{1/2}$ are Fermi–Dirac integrals of order $-1/2$ and 1/2, and the normalized energies are

$$\eta_\pm(x)=[\mu_\pm-E_S(x)]/k_BT_L, \tag{3.3}$$

in which μ_+ and μ_- are the Fermi levels associated with $+$ and $-$ stream, respectively, and $E_S(x)$ is the lowest subband energy of our model device. The Fermi levels depend on whether a stream comes from the source or from the drain contact.[9]

For the source injection, we solve Eqs. (2.1a) and (2.1b) with the backscattering coefficients in Eqs. (3.1), where the normalized energies are

$$\eta_+(x)=\eta_S(x)=[\mu_S-E_S(x)]/k_BT_L, \tag{3.4a}$$

and

$$\eta_-(x)=\eta_S(x_{\max})=[\mu_S-E_S(x_{\max})]/k_BT_L, \tag{3.4b}$$

where μ_S is the Fermi level of the source contact and $x_{\max}$ is the position of the top of the source barrier. In the region $x_{\max}<x<L$ where $\varepsilon_x<0$ in Fig. 4, $\eta_-(x)$ can be any finite value because there is no source-injected negative stream in the ballistic limit. Thus, Eq. (3.4b) causes no error in the ballistic limit. In a similar way, we solve Eqs. (2.1a) and (2.1b) for the drain injection with

$$\eta_+(x)=\eta_D(x_{\max})=[\mu_D-E_S(x_{\max})]/k_BT_L, \tag{3.5a}$$

and

$$\eta_-(x)=\eta_D(x)=[\mu_D-E_S(x)]/k_BT_L, \tag{3.5b}$$

where μ_D is the Fermi level of the drain contact.

To solve Eqs. (2.1a) and (2.1b), we need to specify (1) hierarchy closure assumptions on the average velocities of source and drain injections $\langle \nu_x \rangle_S^{\pm}$ and $\langle \nu_x \rangle_D^{\pm}$, and (2) boundary conditions for source and drain injections.

C. Ballistic hierarchy closure approximations for streams under acceleration

Figure 6 depicts the development of ballistic peaks along the channel of the model device,[9] and Fig. 7 shows the corresponding average velocity profiles under bias. Figure 6 implies that in the ballistic limit, the distribution function approaches a Dirac delta function, and can be written as (assuming parabolic band structure)

$$f(x,\vec{p}) = g(x) \times \delta(\vec{p} - \hat{x} p_{x\,\max}), \tag{3.6}$$

where

$$p_{x\,\max} = \sqrt{2 m_t^* [E_{\max} - E_S(x)]}, \tag{3.7}$$

and $E_{\max}$ is the maximum of $E_S(x)$ (Fig. 4) and m_t^* is the transverse effective mass of ellipsoidal valleys of Si. As shown in Fig. 7, in the limit where the δ-peak approximation applies, the distribution in Eq. (3.6) yields

$$\langle \nu_x \rangle = \sqrt{\langle \nu_x^2 \rangle} = \cdots = \sqrt[\ell]{\langle \nu_x^{\ell} \rangle} = \frac{p_{x\,\max}}{m_t^*}, \tag{3.8}$$

where ℓ is the order of moments. Consequently, Eq. (3.8) allows us to terminate the hierarchy of macroscopic moments. This is analogous to Baraff's maximum anisotropy closure for the spherical harmonics expansion of the distribution function.[12]

We build ballistic closures for $\langle \nu_x \rangle_S^{\pm}$ and $\langle \nu_x \rangle_D^{\pm}$ based on the above argument. In $0 < x < x_{\max}$, only J_D^- experiences acceleration and in $x_{\max} < x < L$, only J_S^+ does. Hence, the following closure assumptions can apply:

$$\langle \nu_x \rangle_S^+ = \begin{cases} \tilde{\nu}_T[\eta_S(x)] & 0 < x < x_{\max} \\ \sqrt{\tilde{\nu}_T^2[\eta_S(x_{\max})] + \dfrac{2[E_{\max} - E_S(x)]}{m_t^*}} & x_{\max} < x < L \end{cases}, \tag{3.9a}$$

$$\langle \nu_x \rangle_S^- = \tilde{\nu}_T[\eta_S(x)] \quad 0 < x < x_{\max}, \tag{3.9b}$$

$$\langle \nu_x \rangle_D^+ = \tilde{\nu}_T[\eta_D(x)] \quad x_{\max} < x < L, \tag{3.9c}$$

and

$$\langle \nu_x \rangle_D^- = \begin{cases} \sqrt{\tilde{\nu}_T^2[\eta_D(x_{\max})] + \dfrac{2[E_{\max} - E_S(x)]}{m_t^*}} & 0 < x < x_{\max} \\ \tilde{\nu}_T[\eta_D(x)] & x_{\max} < x < L \end{cases}. \tag{3.9d}$$

The degenerate thermal velocity $\tilde{\nu}_T(\eta)$ for a two-dimensional electron gas (2DEG) is given as[13]

$$\tilde{\nu}_T(\eta) = \sqrt{\frac{2 k_B T_L}{\pi m_t^*} \frac{\mathscr{F}_{1/2}(\eta)}{\ln(1 + e^{\eta})}}. \tag{3.9e}$$

There are two things worth noting in Eqs. (3.9). First, the closures in Eqs. (3.9a) and (3.9d) reduce to near-equilibrium closures at $x_{\max}$ because $E_{\max} - E_S(x) = 0$ capturing the injection limit properly, but become high-field ballistic closures satisfying Eq. (3.8) where the accelerated carriers develop to a δ peak away from $x_{\max}$. Second, $\langle \nu_x \rangle_S^-$ in $x_{\max} < x < L$ and $\langle \nu_x \rangle_D^+$ in $0 < x < x_{\max}$ are not specified because in the ballistic limit, J_S^- and J_D^+ do not exist in the respective regions.

D. Boundary conditions

To solve Eqs. (2.1a) and (2.1b) self consistently with the Poisson equation, the carrier densities and flux densities of the streams coming into the device should be specified. Those quantities are directly obtained from the distributions given at the contacts. For the source injection, the boundary distributions of the incoming fluxes are

$$f_S(x=0,\ p_x>0) = \frac{1}{1 + \exp\{[E(x=0) - \mu_S]/k_B T_L\}} \tag{3.10a}$$

at the source contact, and

$$f_S(x=L,\ p_x<0) = 0 \tag{3.10b}$$

at the drain contact if perfect absorbing contacts are assumed.[9] In Eqs. (3.10), the total energy of a 2D electron in the $x-y$ plane (due to the vertical confinement in z in our model device) is

$$E(x) = E_S(x) + \frac{p_x^2 + p_y^2}{2 m_t^*}. \tag{3.11}$$

For the drain injection, the boundary distribution given at the drain contact is

$$f_D(x=L,\ p_x<0) = \frac{1}{1 + \exp\{[E(x=L) - \mu_D]/k_B T_L\}}, \tag{3.12a}$$

and at the source contact, it is

$$f_D(x=0,\ p_x>0) = 0. \tag{3.12b}$$

Then, integrating Eqs. (3.10) and (3.12), we obtain the boundary conditions, which are

$$n_S^+(0)=\frac{m_t^* k_B T_L}{2\pi\hbar^2}\log\{1+\exp[\eta_S(0)]\}, \tag{3.13a}$$

$$J_S^+(0)=n_S^+(0)\tilde{\nu}_T[\eta_S(0)], \tag{3.13b}$$

$$\text{and} \qquad J_S^-(L)=0, \tag{3.13c}$$

for the source injection, and

$$n_D^-(L)=\frac{m_t^* k_B T_L}{2\pi\hbar^2}\log\{1+\exp[\eta_D(L)]\}, \tag{3.14a}$$

$$J_D^-(L)=n_D^-(L)\tilde{\nu}_T[\eta_D(L)], \tag{3.14b}$$

$$\text{and} \qquad J_D^+(0)=0, \tag{3.14c}$$

for the drain injection, respectively.

In principle, we solve Eqs. (2.1a) and (2.1b) with Eqs. (3.13) for the source injection, and with Eqs. (3.14) for the drain injection. However, we convert the extended one-flux equations and the boundary conditions into a drift-diffusion form and use Scharfetter–Gummel discretization method.[14]

IV. DRIFT-DIFFUSION EQUATION FOR BALLISTIC MOSFETS

A. Conversion into drift-diffusion equation

By subtracting and adding Eqs. (2.1a) and (2.1b), we obtain

$$\frac{dJ}{dx}=0, \tag{4.1}$$

$$\text{and} \qquad J=-\frac{\xi-\xi'}{\xi+\xi'}\nu_T N-\frac{\nu_T}{\xi+\xi'}\frac{dN}{dx}, \tag{4.2}$$

where the quantities J and N are defined as

$$J\equiv J^+-J^-, \quad [1/\text{cm}^2\,\text{s}] \tag{4.3}$$

$$\text{and} \qquad N\equiv(J^++J^-)/\nu_T \quad [\text{cm}^{-3}] \tag{4.4}$$

The thermal velocity ν_T given in Eq. (2.3) just defines the unit of N. Note that J denotes the net flux density but that N is *not* the actual carrier density but simply represents the sum of $J^\pm$ in the unit of carrier density. Thus, Eq. (4.2) is not restricted to the carriers moving at a fixed velocity ν_T. Using Eqs. (2.1c) and (2.1d) with the implementation of degenerate statistics, Eq. (4.2) can be expressed as a drift-diffusion equation

$$J=-\text{M}\varepsilon_x N-\Delta\frac{dN}{dx}. \tag{4.5a}$$

The equivalent mobility M and diffusivity Δ are defined as

$$M\equiv\frac{\nu_T}{2\xi_0\dfrac{kT_L/q}{F_{\text{deg}}}+|\varepsilon_x|}, \quad [\text{cm}^2/\text{Vs}] \tag{4.5b}$$

$$\text{and} \qquad \Delta\equiv\frac{kT_L}{qF_{\text{deg}}}\text{M}, \quad [\text{cm}^2/\text{s}] \tag{4.5c}$$

$$\text{where} \qquad F_{\text{deg}}=\begin{cases}F_{\text{deg}}^+(\eta_+) & \varepsilon_x>0\\ F_{\text{deg}}^-(\eta_-) & \varepsilon_x<0\end{cases}. \tag{4.5d}$$

Although Eq. (4.5a) is in a drift-diffusion form, it describes spatial variation of flux densities due to transmission and reflection as in the original one-flux equations. In the near-equilibrium diffusive limit, Eq. (4.2) reduces to a drift-diffusion equation and the equivalent mobility and diffusivity become the low-field mobility and corresponding diffusivity.[6] However, when $\xi_0=0$, Eqs. (4.5) describe ballistic transport. Equation (4.5c) is an equivalent Einstein relation under degenerate conditions, which originates from the equilibrium Fermi–Dirac distribution associated with field backscattering (see Appendix B). For degenerate bulk semiconductors, the Einstein relation is[15]

$$\frac{D}{\mu}\equiv\frac{k_B T_L}{q}\left(\frac{n}{dn/d\eta}\right)^{-1}, \tag{4.6}$$

which would yield the degeneracy factor for the 2D carriers in our model device as

$$F_{\text{deg}}=\frac{n}{dn/d\eta}=\frac{\mathscr{F}_{-1}(\eta)}{\mathscr{F}_0(\eta)}=\frac{e^\eta}{(1+e^\eta)\ln(1+e^\eta)}, \tag{4.7}$$

where n is the carrier density. However, the degeneracy factors in Eq. (3.2) imply that

$$F_{\text{deg}}^\pm=\frac{\mathscr{F}_{-1/2}(\eta_\pm)}{\mathscr{F}_{1/2}(\eta_\pm)}=\frac{J^\pm}{dJ^\pm/d\eta_\pm}. \tag{4.8}$$

Equation (4.8) reduces to Eq. (4.7) when the degeneracy associated with the average velocities is independent of position, which is true in uniform bulk semiconductors.

B. Boundary conditions

Using Eqs. (4.3) and (4.4), the boundary conditions for Eqs. (4.1) and (4.5a) are expressed as, at the source contact

$$N(0)[\nu_T-\text{M}\varepsilon_x(0)]-\Delta\left.\frac{dN}{dx}\right|_0=2J^+(0), \tag{4.9a}$$

and at the drain contact

$$N(L)[\nu_T+\text{M}\varepsilon_x(L)]+\Delta\left.\frac{dN}{dx}\right|_L=2J^-(L), \tag{4.9b}$$

where $J^+(0)$ and $J^-(L)$ are given in Eqs. (3.13) for the source injection and Eqs. (3.14) for the drain injection. We solve Eqs. (4.1) and (4.5) for the source injection using the Scharfetter-Gummel discretization technique[14] with the boundary conditions given by Eqs. (3.13) and (4.9) to obtain $N_S(x)$ and $J_S(x)$, i.e., J_S^+ and J_S^- and then using the closure assumptions in Eqs. (3.9a) and (3.9b), we get the carrier densities of source injection n_S^+ and n_S^- because $J_S^\pm=n_S^\pm\langle\nu_x\rangle_S^\pm$. Similarly, we solve Eqs. (4.1) and (4.5) for the drain injection using Eqs. (3.14) and (4.9) to obtain J_D^+ and J_D^- and then n_D^+ and n_D^-. The total carrier density is then

$$n=n_S^++n_S^-+n_D^++n_D^-, \tag{4.10}$$

and the total flux net density is

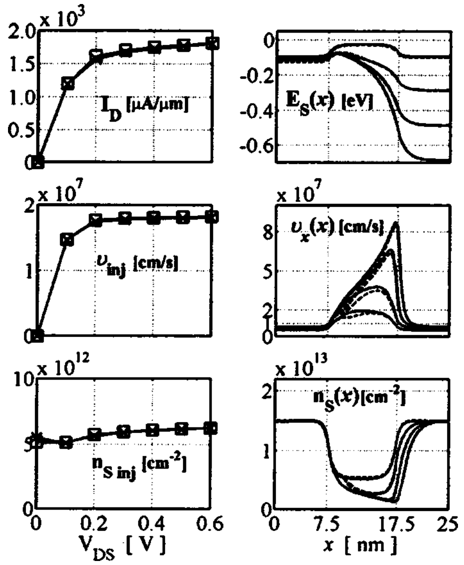

FIG. 8. The I-V characteristics and injection quantities vs V_{DS} (left column), and the profiles of the first subband energy, carrier velocity, and the charge density along the position (right column). The results of the ballistic drift-diffusion equation (x or dashed lines) perfectly match the results of the ballistic BTE from Ref. 9 (square or solid lines).

$$J=(J_S^+-J_S^-)+(J_D^+-J_D^-). \tag{4.11}$$

C. Results

The I_D-V_{DS} characteristics and injection quantities versus drain bias (injection velocity and injection charge density at the top of the barrier) are plotted in the left column of Fig. 8. They are in excellent agreement with the solution of the ballistic BTE[9] showing that the closure approximations in Eqs. (3.9) do not cause error in capturing the injection limit. We then plot profiles of internal quantities (the first subband profile, internal velocity, and charge density versus position) in the right column of Fig. 8. Also, they show excellent overall agreement with the solution of the ballistic BTE except the tolerable errors in the low-field region after the barrier where the delta-peak assumption in Eq. (3.8) is not valid. Thus, the results show that a macroscopic transport model based on the moments of the BTE can describe carrier transport in the ballistic limit.

V. CONCLUSION

We derived and solved a drift-diffusion equation in the ballistic limit for a nanoscale MOSFET. The equation is developed extending McKelvey's one-flux method by (1) treating carrier injection from the source and drain separately, (2) introducing hierarchy closure approximations for the streams under acceleration, and (3) including degenerate carrier statistics involving a properly defined Einstein relation. The results show that a moment-based macroscopic transport model can describe ballistic transport in excellent agreement with the solution of the ballistic BTE with no fitting parameters.

The development of the ballistic macroscopic equation was relatively simple because (1) we were able to treat injection from the source and drain separately due to the linearity of the ballistic BTE and (2) the hierarchy closure approximations were independent of scattering. When scattering is present, however, those two simplifications should be reexamined. First, carrier–carrier scattering under degenerate conditions may couple the source and the drain injections (the BTE becomes nonlinear) weakening the assumption of separating injections in principle. Second, the scattering and the accelerating electric field brings complicated transport because the strength of scattering depends on the carriers' kinetic energy, which again depends on the interplay of the accelerating field and the impeding scattering. Describing these phenomena in an acceptable error range still remains the most difficult challenge in developing a macroscopic model valid in the high-field quasiballistic regime.

ACKNOWLEDGMENTS

This work is supported by the National Science Foundation through the Distributed Center for Advanced Electronics Simulations (DesCArtES) and by the Semiconductor Research Foundation (SRC).

APPENDIX A: DERIVATION OF ONE-FLUX EQUATIONS

We present a brief but proper derivation of Eqs. (2.1a)–(2.1d) from the Boltzmann transport equation (BTE). For 1D transport along the x direction as in our model device, the steady-state BTE is

$$\nu_x\frac{\partial f}{\partial x}-q\varepsilon_x\frac{\partial f}{\partial p_x}=\left.\frac{\partial f}{\partial t}\right|_{\text{coll}}, \tag{A1}$$

where the carrier distribution as a function of x and $\vec{p}=(p_x,\ p_y,\ p_z)$ is $f=f(x,\vec{p})$. Equations (2.1a)–(2.1d) are derived taking partial averages of Eq. (A1) over the two subdomains of the momentum space (1) $\Omega_+=\{\vec{p}|p_x>0\}$ for $+$ stream and (2) $\Omega_-=\{\vec{p}|p_x<0\}$ for $-$ stream. The whole momentum space is $\Omega=\Omega_+\cup\Omega_-$. The averages of the *flux* term of Eq. (A1) over $\Omega_\pm$ yield the spatial variations of $J^\pm$, i.e.,

$$\begin{aligned}\frac{1}{V}\sum_{\Omega_\pm}\ \nu_x\frac{\partial f}{\partial x}&=\frac{d}{dx}\left(\frac{1}{V}\sum_{\Omega_\pm}\ \nu_x f\right)\\&=\frac{d}{dx}(\pm J^\pm),\quad\text{(flux terms)}\end{aligned} \tag{A2}$$

where V is a normalization volume and J^- is defined positively. Applying the chain rule, $\partial f/\partial p_x=\partial f/\partial E\ \partial E/\partial p_x$ and the identity, $\partial E/\partial p_x=\nu_x$, to the *field* term of Eq. (A1), we obtain

$$\frac{1}{V}\sum_{\Omega_\pm}\ q\varepsilon_x\frac{\partial f}{\partial p_x}=q\varepsilon_x\left(\frac{1}{V}\sum_{\Omega_\pm}\ (\nu_x f)\frac{1}{f}\frac{\partial f}{\partial E}\right), \tag{A3}$$

where E is the total carrier energy. Converting the sum over p_x into an integral, we obtain

$$\frac{1}{V}\sum_{\Omega_\pm}\ q\varepsilon_x\frac{\partial f}{\partial p_x}=\pm q\varepsilon_x\frac{1}{2\pi\hbar A}\sum_{p_y,p_z}\ f(p_x=0,\ p_y,\ p_z), \tag{A4}$$

where A is a normalization area of the y-z plane. Note that $f(0,p_y,p_z)$ represents stationary carriers in the x direction, which are generated by the decelerating electric field ε_x (see Fig. 3). Hence, it is reasonable to assume that the distribution associated with a stream under deceleration remains in a near-equilibrium shape as in thermionic emission. In nondegenerate conditions, a hemi-Maxwellian, $f \sim \exp(-E/k_BT_L)$, can be assumed. Then, from Eq. (A3), we obtain

$$\frac{1}{V}\sum_{\Omega_\pm}(\nu_x f)\frac{1}{f}\frac{\partial f}{\partial E} = -\frac{1}{k_BT}\frac{1}{V}\sum_{\Omega_\pm}\nu_x f = \mp\frac{J^\pm}{k_BT}, \tag{A5}$$

or $$\frac{1}{V}\sum_{\Omega_\pm} q\varepsilon_x\frac{\partial f}{\partial p_x} = \mp\frac{q\varepsilon_x}{k_BT}J^\pm. \quad \text{(field terms)} \tag{A6}$$

The averages of the *scattering* term of the BTE are expressed as

$$\frac{1}{V}\sum_{\Omega_\pm}\left.\frac{\partial f}{\partial t}\right|_{\text{coll}} = \pm\left(-\frac{n^+}{\tau^+}+\frac{n^-}{\tau^-}\right), \tag{A7}$$

where $n^\pm$ are carrier densities in ± streams and $\tau^\pm$ are corresponding macroscopic relaxation times associated with backscattering. Although Eq. (A7) can be derived rigorously from the scattering integral of the BTE, the following phenomenological explanation verifies Eq. (A7). The averages of the BTE over $\Omega_\pm$ yield the rate equations for carrier densities $n^\pm$. Thus, the backscattering of $+$ stream decreases n^+ with the rate of n^+/τ^+ but the backscattering of $-$ stream increases n^+ with the rate of n^-/τ^-. Scattering that causes a carrier to remain in the same stream does not appear because it does not change the number of carriers. The sign ± in Eq. (A7) results from the continuity condition

$$\frac{1}{V}\sum_{\Omega}\left.\frac{\partial f}{\partial t}\right|_{\text{coll}} = \frac{1}{V}\sum_{\Omega_+}\left.\frac{\partial f}{\partial t}\right|_{\text{coll}} + \frac{1}{V}\sum_{\Omega_-}\left.\frac{\partial f}{\partial t}\right|_{\text{coll}} = 0, \tag{A8}$$

since scattering neither creates nor destroy carriers (we exclude explicit generation or recombination of carriers). To make Eq. (A7) compatible with the one-flux equations, we define scattering mean-free-paths for ± streams as

$$\lambda^\pm \equiv 1/\xi^\pm = \langle \nu_x\rangle^\pm \tau^\pm. \tag{A9}$$

Further, we assume that $\xi^+ \cong \xi^- \cong \xi_0$, which is valid in near equilibrium. Then, using Eq. (2.2), Eq. (A7) becomes

$$\frac{1}{V}\sum_{\Omega_\pm}\left.\frac{\partial f}{\partial t}\right|_{\text{coll}} = \pm(-\xi_0 J^+ + \xi_0 J^-). \quad \text{(scattering terms)} \tag{A10}$$

From Eqs. (A2), (A6), and (A10), we can obtain Eqs. (2.1a)–(2.1d).

APPENDIX B: DERIVATION OF DEGENERACY FACTORS

We derive Eqs. (3.1a) and (3.1b). In degenerate semiconductors, the near equilibrium distribution f associated with streams under deceleration can be assumed to be

$$f(x,E) = \frac{1}{1+\exp[(E-\mu_\pm)/k_BT_L]}. \tag{B1}$$

Using the property, $\partial f/\partial E = -\partial f/\partial\mu_\pm$, we can see that

$$\sum_{\Omega_\pm}\frac{\partial f}{\partial p_x} = \sum_{\Omega_\pm}\nu_x\frac{\partial f}{\partial E} = -\frac{\partial}{\partial\mu}\left(\sum_{\Omega_\pm}\nu_x f\right) = -\frac{\partial}{\partial\mu}(\pm J^\pm). \tag{B2}$$

For the 2D electrons in our model device, $J^\pm = J_0 \mathscr{F}_{1/2}(\eta_\pm)$,[13] where J_0 is the bias-independent flux density, and $\eta_\pm(x) = [\mu_\pm - E_S(x)]/k_BT_L$. From Eqs. (A3), (B1), and (B2), we can show that

$$F_{\text{deg}}^{\pm} = \frac{\mathscr{F}_{-1/2}(\eta_\pm)}{\mathscr{F}_{1/2}(\eta_\pm)}, \tag{B3}$$

using the property of Fermi–Dirac integral,[16]

$$\frac{\partial}{\partial\mu_\pm}\mathscr{F}_j(\eta_\pm) = \frac{1}{k_BT_L}\mathscr{F}_{j-1}(\eta_\pm).$$

[1] M. Nekovee, B. Geurts, H. M. Bootsand, and M. F. H. Schuurmans, Phys. Rev. B **45**, 6643 (1992).
[2] J.-H. Rhew and M. S. Lundstrom, in J. Computat. Electron. (submitted).
[3] S. E. Laux and M. V. Fischetti, IEEE Electron Device Lett. **9**, 467 (1988).
[4] K. Banoo, M. S. Lundstrom, and R. K. Smith, in 2000 International Conference on Simulation of Semiconductor Processes and Devices: SISPAD2000, Sheration Seattle Hotel and Towers, Seattle, WA, 2000.
[5] J. P. McKelvey, R. L. Longini, and T. P. Brody, Phys. Rev. **123**, 51 (1961).
[6] W. Shockley, Phys. Rev. **125**, 1570 (1962).
[7] M. S. Lundstrom, IEEE Electron Device Lett. **18**, 361 (1997).
[8] M. Alam, M. Stettler, and M. S. Lundstrom, Solid-State Electron. **36**, 263 (1993).
[9] J.-H. Rhew, Z. Ren, and M. S. Lundstrom, Solid-State Electron. (submitted).
[10] M. S. Lundstrom, *Fundamentals of Carrier Transport* (Cambridge University, Cambridge, England, 2000).
[11] S. Tanaka and M. S. Lundstrom, IEEE Trans. Electron Devices **42**, 1806 (1995).
[12] G. A. Baraff, Phys. Rev. A **111**, A26 (1964).
[13] F. Assad, Z. Ren, D. Vasileska, S. Datta, and M. S. Lundstrom, IEEE Trans. Electron Devices **47**, 232 (2000).
[14] D. L. Scharfetter and D. L. Gummel, IEEE Trans. Electron Devices **16**, 64 (1969).
[15] N. Ashcroft and N. Mermin, *Solid State Physics* (Saunders College Publishing, Orlando, Florida, 1976).
[16] J. S. Blakemore, *Semiconductor Statistics* (Macmillian, New York, 1962).